ADVANCED MATERIALS

www.advmat.de

Autonomous Ultrafast Self-Healing Hydrogels by pH-Responsive Functional Nanofiber Gelators as Cell Matrices

Jasmina Gačanin, Jana Hedrich, Stefanie Sieste, Gunnar Glaßer, Ingo Lieberwirth, Corinna Schilling, Stephan Fischer, Holger Barth, Bernd Knöll, Christopher V. Synatschke, and Tanja Weil**

The synthesis of hybrid hydrogels by pH-controlled structural transition with exceptional rheological properties as cellular matrix is reported. "Depsi" peptide sequences are grafted onto a polypeptide backbone that undergo a pH-induced intramolecular O–N–acyl migration at physiological conditions affording peptide nanofibers (PNFs) as supramolecular gelators. The polypeptide–PNF hydrogels are mechanically remarkably robust. They reveal exciting thixotropic behavior with immediate in situ recovery after exposure to various high strains over long periods and self-repair of defects by instantaneous reassembly. High cytocompatibility, convenient functionalization by coassembly, and controlled enzymatic degradation but stability in 2D and 3D cell culture as demonstrated by the encapsulation of primary human umbilical vein endothelial cells and neuronal cells open many attractive opportunities for 3D tissue engineering and other biomedical applications.

The extracellular matrix (ECM) has been optimized during evolution and forms a complex, supportive environment for cells providing mechanical and biochemical cues, and enabling cells to communicate.[1] There is an emerging interest to design synthetic materials that serve as artificial matrices stimulating cell growth and division,[2] providing therapeutic options, such as in tissue engineering,[3] cell printing,[4] and in regenerative medicine.[5] Nanofiber-forming peptides have been extensively studied in the biomaterials field, as they mimic the fibrous part of the ECM morphology formed by proteins such as collagen and support the survival and growth of cells when applied as coatings or 3D matrices.[6] Short peptide sequences, such as the RADA-16 peptide, peptide amphiphiles, and Fmoc-functionalized oligopeptides are promising artificial cell supports.[7] These materials have potential applications in regenerating both hard and soft tissues.[8] However, their strong tendency to form fibrous aggregates under a broad range of conditions has been problematic, e.g., during chemical modification and purification, which prompted the implementation of induced fiber formation by external triggers.[9] Furthermore, the natural ECM is heterogeneous and contains covalent polymers such as proteoglycans in addition to supramolecular protein fibers. Consequently, purely supramolecular hydrogels often lack long-term stability in cell media and are mechanically fragile. Hybrid materials combining both covalent and supramolecular components may address these needs. Additionally, implementing injectability and self-healing properties is essential for less invasive applications to limit injury to the patient.[10] Current approaches for achieving injectable hydrogels include thermogelation, dynamic-covalent bonds, and host–guest interactions.[11] For biomedicinal applications, biocompatibility of the hydrogel and its degradation products represent a key concern, and reactive groups within the gel can be problematic. Therefore, natural biopolymers such as DNA or self-assembling peptides have been proposed as cross-linkers enabling reversible gelation.[12] However, the design of hydrogels that could serve as biocompatible and biodegradable cell matrices with sufficient stability during cultivation, combined with controlled and rapid gelation as well as excellent self-healing properties, are still elusive.

Herein, we propose hybrid hydrogels providing a soft polypeptide matrix combined with covalently attached poly(ethylene gylcol) (PEG) chains and short self-assembling peptide motifs for pH-induced gelation through formation of a peptide nanofiber (PNF) network. These materials may provide high biocompatibility as they are constructed mostly from amino

J. Gačanin, Dr. J. Hedrich, S. Sieste, G. Glaßer, Dr. I. Lieberwirth, Dr. C. V. Synatschke, Prof. T. Weil
Max Planck Institute for Polymer Research
55128 Mainz, Germany
E-mail: synatschke@mpip-mainz.mpg.de; weil@mpip-mainz.mpg.de, Tanja.Weil@uni-ulm.de

J. Gačanin, S. Sieste, Prof. T. Weil
Institute of Inorganic Chemistry I
University of Ulm
89081 Ulm, Germany

C. Schilling, Prof. B. Knöll
Institute of Physiological Chemistry
University of Ulm
89081 Ulm, Germany

S. Fischer, Prof. H. Barth
Institute of Pharmacology and Toxicology
University of Ulm Medical Center
89081 Ulm, Germany

The ORCID identification number(s) for the author(s) of this article can be found under https://doi.org/10.1002/adma.201805044.

DOI: 10.1002/adma.201805044

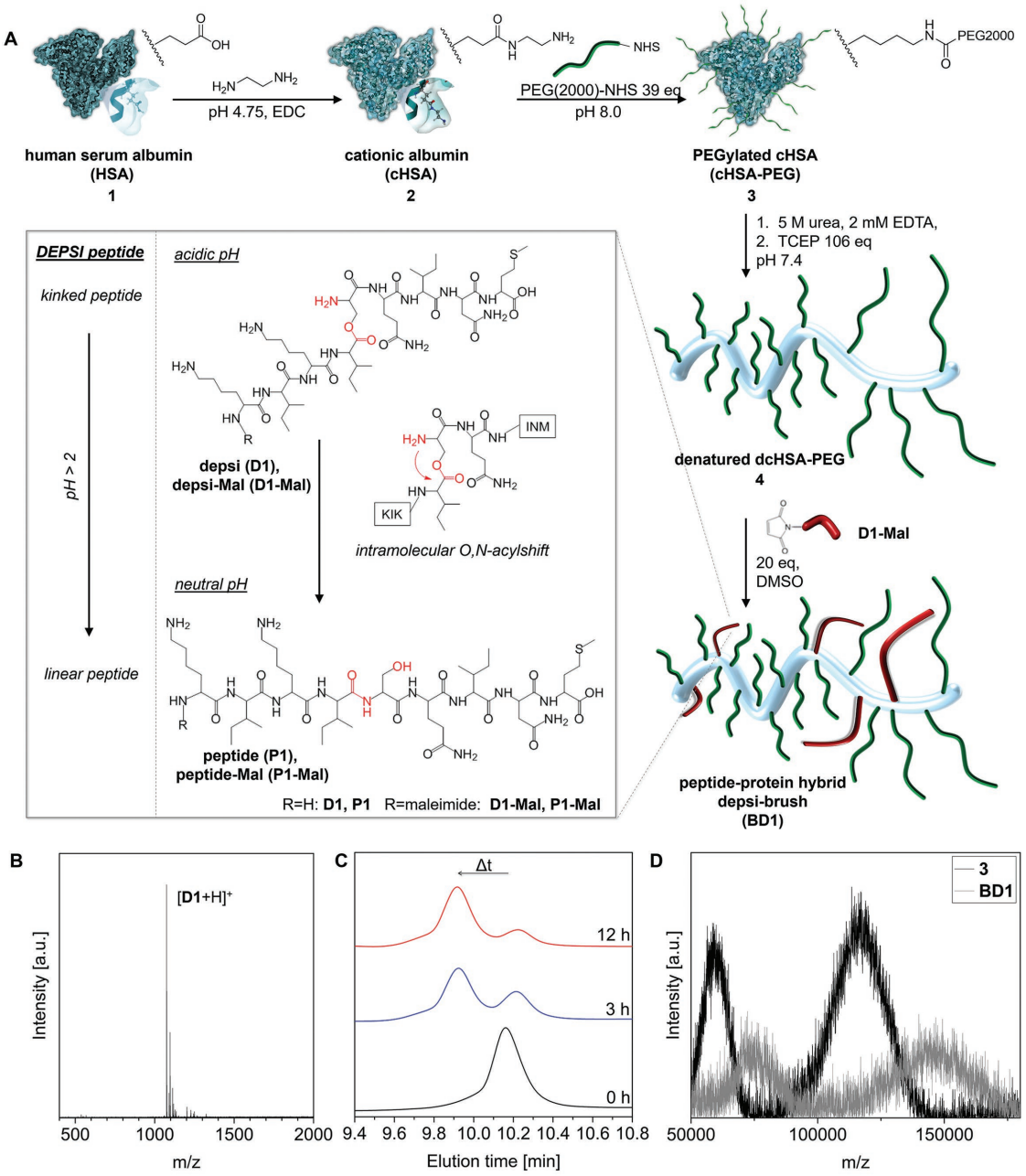

Figure 1. Synthesis of polypeptide–PNF hydrogels. a) Preparation of **BD1**. Box: pH-induced intramolecular O–N–acyl migration of the depsi peptides (**D1, D1-Mal**) yielding linear peptides (**P1, P1-Mal**). b) MALDI FT-ICR MS of **D1.** c) HPLC chromatograms of the conversion of **D1** to **P1** in PBS (1 mg mL^{-1}). d) MALDI-ToF MS of cHSA-PEG (**3**, MW = 115 500 g mol^{-1}) with 22 PEG chains and the polypeptide–depsi copolymer (**BD1**, MW = 145 000 g mol^{-1}) with 20 depsi grafts.

acids and feature ultrafast recovery even after high shear stress over long time periods. They instantaneously recover after passing through a thin injection needle, and they may provide great potential for supporting 2D and 3D cell growth, which offers new avenues for tissue engineering.

The amphiphilic 9mer peptide sequence KIKISQINM (**P1**) was designed as a supramolecular cross-linker. This short peptide is amphiphilic and has a strong tendency to instantaneously form stable cross β-sheet peptide nanofibers (PNFs) in aqueous solution even at low pH conditions (Figure S8, Supporting Information). Furthermore, it provides a central serine residue, which is crucial for preparing the respective depsi sequence KIKI-(COO)-SQINM, **D1**. To selectively trigger self-assembly and to facilitate purification of unreacted peptide at low pH, the depsi peptide version of **P1**, **D1**, was synthesized. **D1** features an ester bond in the main chain and a kinked structure unable to self-assemble into PNFs.[13] Upon increasing the pH to neutral, an intramolecular O–N–acyl migration occurs converting the ester into the peptide bond, which linearizes the depsi peptide and enables instantaneous PNF formation (**Figure 1**A, box).

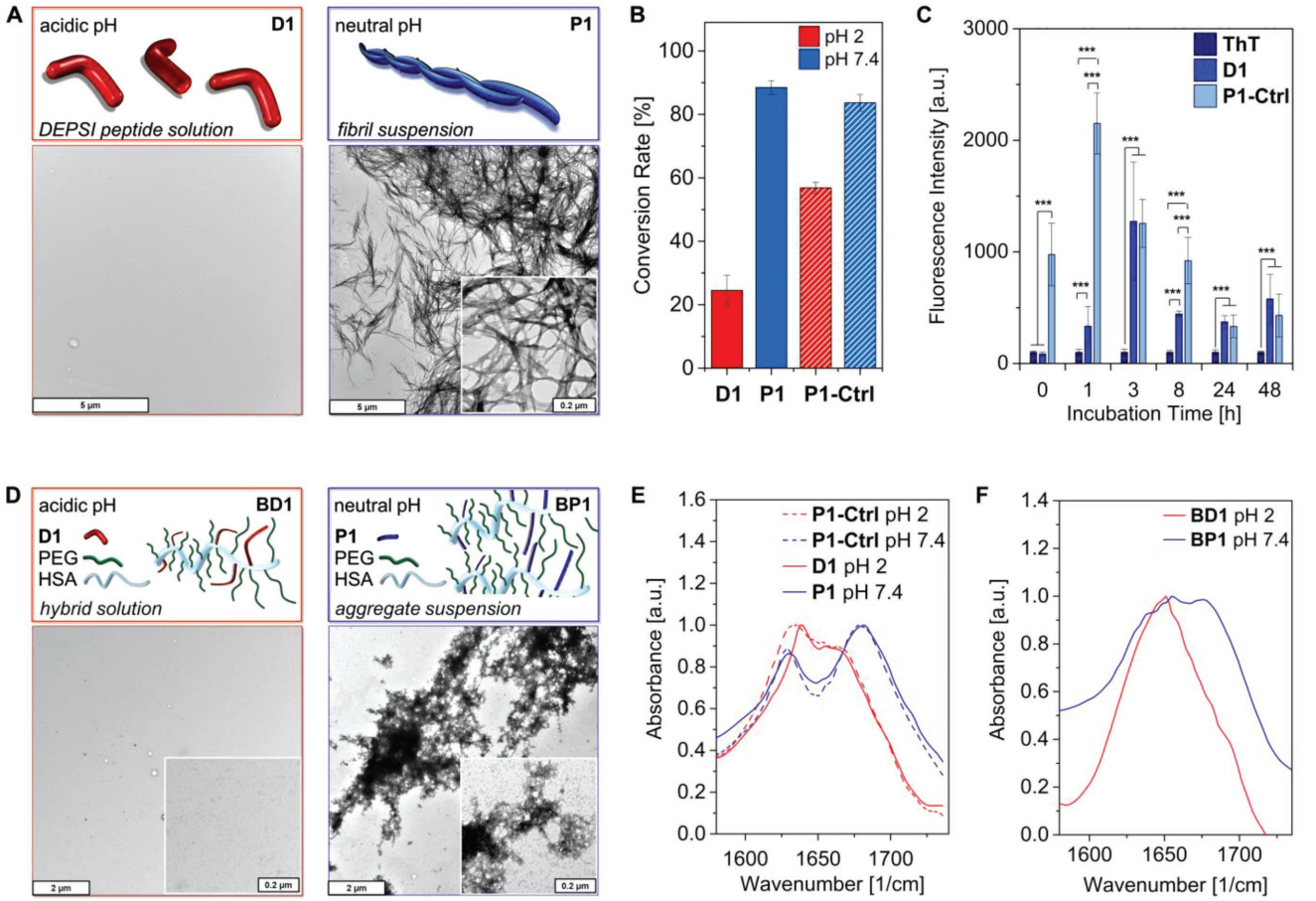

Figure 2. pH responsive PNF formation. a) TEM images of **D1** (1 mg mL^{-1}) incubated at acidic or physiological pH. Scale bars are 5 µm and 200 nm (inset). b) Conversion rates of **D1** and **P1-Ctrl** into PNFs after incubation at acidic or neutral pH (1 mg mL^{-1}). Mean ± s.d. (n = 3). c) ThT assay of **D1** and **P1-Ctrl** after incubation at neutral pH (1 mg mL^{-1}) at different time points. The ThT fluorescence emission was recorded at λ_{em} = 488 nm (λ_{ex} = 440 nm) with 10 nm bandwidths and multiple reads per well (3 × 3). Data are presented as mean ± s.d. ($n \geq 3$), with nine measurements of the same well at different positions. One-way ANOVA followed by Tukey's multiple comparisons test was performed ($P < 0.05$ (*), $P < 0.01$ (**), and $P < 0.001$ (***). d) TEM images of **BD1** (1 mg mL^{-1}) incubated at acidic or physiological pH. Scale bars are 2 µm and 200 nm (insets). e) ATR FT-IR spectra of **D1** and **P1-Ctrl** at acidic or neutral pH (1 mg mL^{-1}). f) ATR FT-IR spectra of **BD1** in acidic or neutral pH (1 mg mL^{-1}).

The depsi peptide **D1** was synthesized by solid phase peptide synthesis (SPPS) under Fmoc-protection combined with the O–acyl isopeptide method (Scheme S1, Supporting Information) and purified by reverse-phase HPLC. MALDI FT-ICR MS showed the expected m/z value of the desired product (Figure 1B). The intramolecular O–N–acyl migration in **D1** was induced at neutral pH, and PNF formation was analyzed by high-performance liquid chromatography (HPLC), transmission electron microscopy (TEM), emission spectroscopy, and Fourier-transform infrared spectroscopy (FT-IR) measurements. In HPLC, the retention times shifted from 10.18 min for **D1** (Figure S9A, Supporting Information) to 9.90 min for **P1** (KIKISQINM, Figure 1C). Note that **P1** was formed from depsi peptide **D1**, whereas the reference peptide **P1-Ctrl** of the same KIKISQINM sequence was directly prepared by SPPS.

P1 forms PNFs exceeding several micrometers in length and 11.30 ± 1.26 nm in diameter, whereas no PNF formation occurred at low pH (**Figure 2**A). The conversion rate measures the amount of soluble peptide that is converted to PNFs. At neutral pH, high conversion rates of 88.5 ± 2.2% and 83.7 ± 2.6% were obtained for **D1** and **P1-Ctrl**, respectively (Figure 2B). At acidic pH, only **P1-Ctrl** assembled into PNFs with 56.9 ± 1.8%, whereas **D1** showed only low aggregation tendency of 24.5 ± 4.7% and no PNFs were visible in TEM, confirming the pH-dependent PNF formation. Cross β-sheet structures in PNFs from **P1** and **P1-Ctrl** at neutral pH were characterized by the blueshifted emission of Thioflavin T (ThT, Figure 2C)[14] and the minimum in the circular dichroism spectra at around 216 nm (Figure S10, Supporting Information). Also, FT-IR spectroscopy of freeze-dried **D1** at low pH gave signals in the amide I band region between 1590 and 1735 cm^{-1} (Figure 2E) and a maximum peak at 1638–1639 cm^{-1} related to unordered structures, whereas the linear peptide **P1-Ctrl** showed a maximum peak at 1634–1636 cm^{-1} corresponding to β-sheets.[15] At pH ≈7, **D1** was converted to **P1** and a new maximum signal at 1680–1682 cm^{-1} and a second signal at 1630 cm^{-1} appeared indicating β-sheet structures.

For the hybrid hydrogel, maleimide-functionalized **D1** (**D1-Mal**, Figure S3, Supporting Information) was conjugated to the long polypeptide backbone of denatured human

serum albumin (HSA) providing in vivo biocompatibility and biodegradability. The synthetic route for depsi-grafted polypeptide **BD1** is shown in Figure 1A. First, HSA (**1**) was converted to cationized HSA (cHSA, **2**) to introduce primary amine groups facilitating interactions with cellular membranes.[16] Subsequently, about 22 poly(ethylene glycol) (PEG) chains (MW = 2000 Da) were conjugated to cHSA that bind water molecules and impart higher stability to afford cHSA-PEG (**3**).[17] Denaturation of **3** proceeded in concentrated urea buffer followed by the reduction of all disulfide bridges into reactive sulfhydryl groups yielding **4** with grafted PEG side chains. Then, **4** was reacted with **D1-Mal** yielding depsi-grafted copolymer **BD1** (Figure 1A) with about 20 depsi peptides per polypeptide chain (145 000 m/z, Figure 1D).

The product was well soluble in acidic water facilitating characterization and purification from unreacted components by ultrafiltration. Structural rearrangements from soluble copolymer **BD1** to **hydrogel 1 (H1)** with PNFs as supramolecular gelators were triggered by the pH-induced O–N–acyl migration of grafted **D1** peptides. Upon incubation at neutral pH, ThT active aggregates were obtained and PNFs were clearly visible in TEM (Figure 2D and Figure S12, Supporting Information). However, at low pH, no aggregate formation was detected in TEM images (Figure 2D). These results indicate successful transfer of the aggregation behavior of **D1** to the copolymer **BD1**. FT-IR spectroscopy of freeze-dried **BD1** at low or neutral pH revealed in the amide I band region signals from 1590 to 1735 cm^{-1} and α-helical structures at 1655 cm^{-1} from the α-helical-rich polypeptide backbone. At neutral pH, new bands at 1680 cm^{-1} appeared indicating the presence of anti-parallel β-sheet structures (Figure 2F). The corresponding copolymer **BP1-Ctrl** without the pH-switch was also prepared by conjugating the linear model peptide **P1-Ctrl-Mal** (Figure S4, Supporting Information) to the polypeptide backbone **4**. **BP1-Ctrl** showed immediate aggregation in all solvents and at any pH, making purification from, e.g., unreacted peptide monomers impossible (Figure S13, Supporting Information).

At 4 wt% mass concentration, instantaneous gelation was observed in phosphate buffer solution (PBS, pH 7.4) yielding **H1** with a highly porous structure and mean pore sizes of 11 ± 3.5 µm, as observed by scanning electron microscopy (SEM, Figure S15, Supporting Information). Convenient functionalization by simply mixing (copolymerization) **D1** (18 eq), rhodamine dye labelled **D1-Rho** (2 eq, Figure S5, Supporting Information), and **BD1** afforded the respective fluorescently labeled PNFs inside the hydrogel **H3**. Confocal laser scanning microscopy (CLSM) (**Figure 3**A and Figures S16–S18, Supporting Information) showed homogeneous fluorescent staining throughout the material highlighting the opportunity to introduce functionalities into the hydrogels by simply mixing free and functionalized depsi peptide during the gelation process.

The mechanical properties of **H1** were investigated first in a time-sweep experiment (Figure S19, Supporting Information) with fixed frequency and strain. No crossover was observed, indicating instantaneous gelation during sample preparation (30 s). The mechanical strength of **H1** was in the range of several hundred Pa (G' [≈0.7 kPa], G'' [≈0.04 kPa]) and similar to soft tissues[18] and remained constant over time as no structural rearrangements occurred after gelation. The cross-linked gel behavior was further demonstrated by frequency sweeps (Figure 3B) that showed no frequency dependence for both G' and G'' up to 30 rad s^{-1} and only a small continuous increase without intersection at high frequencies. **H1** maintained its mechanical properties even when exposed to oscillatory strains of 15–20% below which the values of G' and G'' remained constant (Figure 3C). With increasing oscillatory strain, G' decreased gradually, whereas G'' increased slightly for strains above 15% indicating a network structure, which does not collapse abruptly but rather gradually. This is most likely due to the long polypeptide backbone that compensated small strains through conformational changes. At high strains >15%, the β-sheet PNFs break with microfissures that gradually expanded to macro-fractures within the hydrogel network.[19] At a failure strain of ≈41%, a gel-to-sol transition occurred and the material behaved like a viscous fluid (Figure S20, Supporting Information).

Four step-strain sweep experiments up to strains of 1000% immediately followed by a period of low fixed strain (0.1%) were applied (Figure 3D) to evaluate the self-healing capability.[20] Remarkably, even though no resting period was granted after each step-strain experiment, the gels recovered almost immediately upon removal of high shear force. **H1** showed superior ultrafast recovery behavior compared to other thixotropic hydrogels, where G' did not recover to the initial values,[12,21,22] or only after tens of minutes at low shear forces,[22–24] or if resting periods without any strain of ≈30 min were afforded.[12,24] The recovery potential of the PNF cross-linked polypeptide hydrogel was extraordinarily high and immediate reassembly of the liquid solution of **BP1** to the hydrogel occurred within less than 20 s after removal of the liquefying strain, indicating that the broken bonds were immediately and reversibly reformed. A nearly quantitative healing efficiency and recovery occurred directly after removal of high strain (Figure S21A, Supporting Information). Even after being subjected to high strain for consecutively longer periods of time (up to 65 min), the hydrogel reformed almost instantaneously (Figure S21B, Supporting Information) upon removal of the high strain condition. Furthermore, **H1** also rapidly self-heals at a macroscopic scale, as demonstrated by the recovery from cutting and rejoining a piece of gel within 5 min after cutting (Figure S21C, Supporting Information).

Noteworthily, self-healing of the PNF gelators proceeded autonomously without the need for external intervention such as the addition of healing agents or external stimuli.[25] The mechanical properties of **H1** remained mostly unaffected by changes in temperature between 25 and 37 °C (Figure S22, Supporting Information) and the presence of serum proteins (Figure S23, Supporting Information). Gel stiffness was adjustable by the number of **D1** attached to the polypeptide chain: Decreasing the number of **D1** (10 copies of **D1** instead of 20) gave significantly weaker gels (G' ≈0.1 kPa, Figure S24, Supporting Information), while doubling the solid content from 4% to 8%, gel stiffness increased by twofold (G' ≈1.8 kPa, Figure S25, Supporting Information). As shown in Figure 3E, **H1** was injectable as demonstrated by writing the letters "U-U" (≈0.5 cm scale) on a glass slide with a syringe "pen" containing rhodamine colored **H1** as "ink."

H2 containing fluorescently labeled polypeptide backbone **BD1-RITC** was prepared inside a transwell setup and incubated in PBS at 37 °C in the presence or absence of the protease

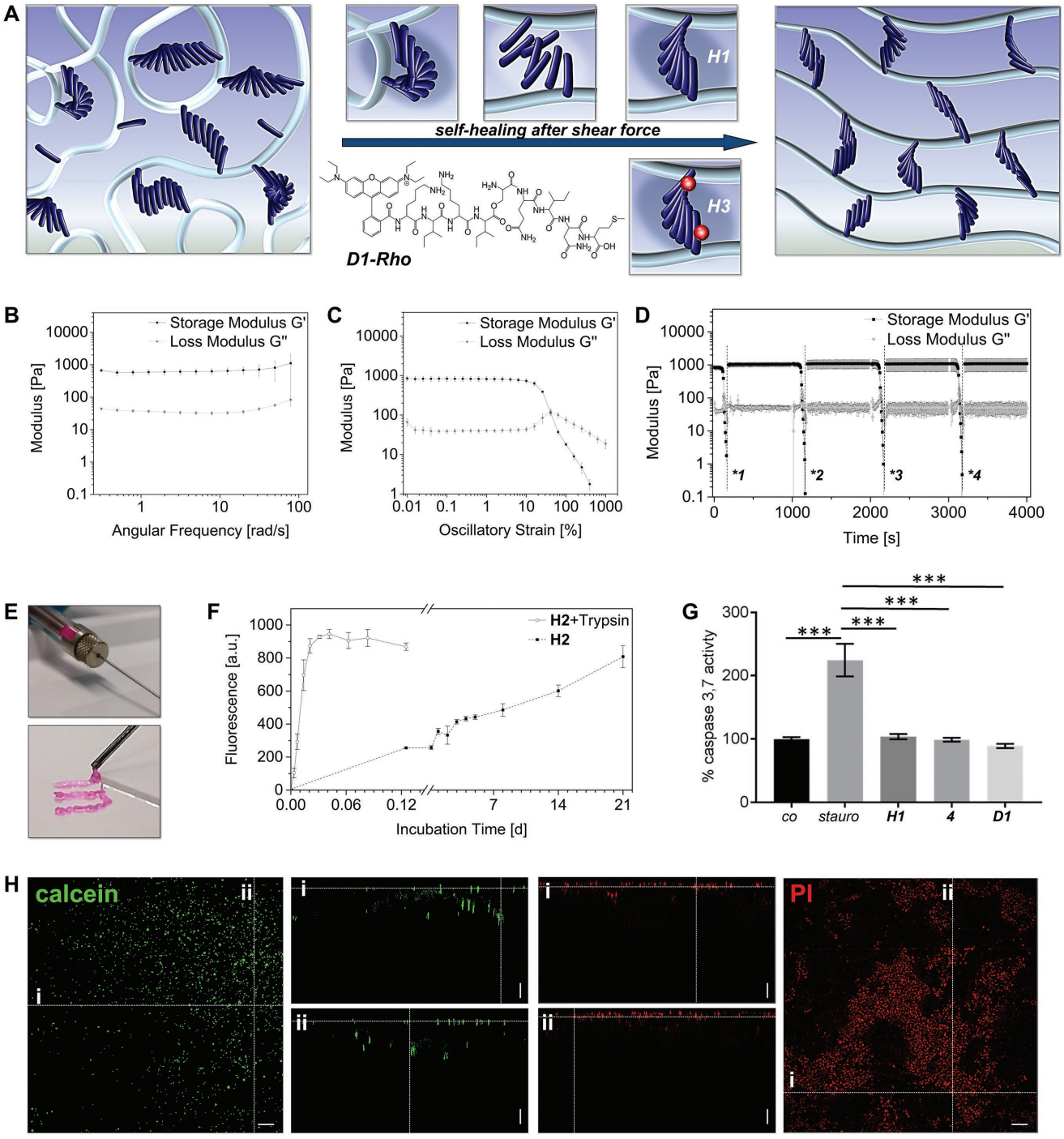

Figure 3. Characterization of polypeptide–PNF hybrid hydrogels (4 wt%). a) Schematic illustration of self-healing due to reassembly of the PNFs cross-linkers after shear stress and functionalization by copolymerization with D1-Rho yielding **H3**. b–d) Rheological characterization of **H1** (25 °C). Mean ± s.d. ($n = 3$). b) Frequency sweep (0.05–100 Hz) with fixed strain (1%). c) Oscillatory strain sweep (0.01–1000%) with fixed frequency (1 Hz). d) Consecutive measurements of oscillatory strain sweeps (0.01–1000%) with fixed frequency (1 Hz), followed by oscillatory time sweep measurements with fixed strain (0.1%) and frequency (1 Hz) demonstrating the thixotropic nature of the hydrogel. e) Injection behavior of **H1**. 3D pattern written with rhodamine B colored **H1** via 0.25 mL Hamilton syringe. f) Degradation of **H2** (25 µL) in the presence of trypsin (0.43 nmol) or in PBS (37 °C) measured by fluorescence intensity of the surrounding medium. Mean ± s.d. ($n = 3$). g) Cell vitality of HUVECs seeded 24 h prior treatment with medium as negative control (co), staurosporine (stauro, positive control, 1×10^{-6} M), **H1** (0.4 mg, 2.8 nmol), **4** (0.35 mg, 2.8 nmol), or **D1** (0.06 mg, 55.9 nmol). Caspase-Glo 3/7 Assay was performed 48 h after cell seeding. Data are plotted as mean ± SEM of four experiments with two replicates each. One-way ANOVA followed by Tukey's multiple comparisons test was performed, *** = $P < 0.001$. h) Migration of HUVECs into **H1**. HUVECs vital and dead were seeded topologically on **H1** and stained with calcein (green, for living cells) or propidium iodid (red, for dead cells), respectively. Orthogonal slices from z-stack confocal images in orthogonal view i and ii show location of cells in **H1** 24 h post seeding. Vital cells migrate into **H1** whereas dead cells localized on top of **H1** and no sinking occurred into the hydrogel. Scale bar is 100 µm.

trypsin. Fluorescence of the surrounding solution was monitored to follow the degradation of the polypeptide backbone (Figure 3F and Figure S26, Supporting Information). **H2** (4%) was rapidly digested within 30–45 min by trypsin (0.43 nmol), but it remained stable in PBS and cell serum for several days indicating its potential as cell matrix. To test the ability of **H1** to support cellular growth, primary human umbilical vein endothelial cells (HUVECs) and primary neuronal cells were used. HUVECs were tested with **H1** (4 wt%), the precursor protein (**4**), and peptide (**D1**) for 24 h. As positive and negative controls, medium (co) and the cell toxin staurosporine (stauro) were used, respectively. HUVECs revealed excellent cell vitality in **H1**, whereas increased caspase 3/7 activity indicative for early apoptosis was only observed in the positive stauro control (Figure 3G). HUVECs were seeded on **H1** and subsequently analyzed by confocal live imaging after 24 h and 7 d. They migrated into **H1**, where they expanded in cell clusters found throughout the gel, and high cell vitality was observed according to the representative orthogonal view of a confocal z-stack (Figure S27, Supporting Information). Viable HUVECs infiltrated **H1** even after topological seeding, while dead cells remained at the top of **H1** without sinking into the gel in a control experiment (Figure 3H). This clearly indicates that cells can migrate along the structure of the protein–peptide scaffold. In contrast, for most known hydrogels, 3D cultures are only observed after resuspension of exogenous cells in the hydrogel precursor solutions.[26] Also, dorsal root ganglion neuronal cells exhibited high viability when cultured on **H1**, comparable to the golden standard Matrigel as a positive control for up to 4 d in vitro (Figure S28, Supporting Information). Additionally, no activation of macrophages in vitro was observed (Figure S29, Supporting Information), demonstrating good cytocompatibility and suggesting low tendency for immune activation.

A nature-inspired cytocompatible hybrid hydrogel was prepared by pH-controlled structural transition of a depsi-peptide-grafted copolymer into a fibrous soft polymer hydrogel. The soluble precursor polymer consisted of denatured HSA grafted with PEG chains for solubility and depsi peptides for controlled gelation and in situ functionalization by coassembly. It was transformed into **H1** with an inner β-sheet fibrous network by convenient pH-induced gelation. The PNF cross-linked hydrogels feature fast gelation, excellent recovery from high strain conditions over multiple cycles, and re-formation after injection as well as macroscopic cutting. These excellent self-healing properties combined with immediate recovery due to the rapid in situ reorganization of the PNF β-sheets are particularly attractive for designing biological matrices that need to withstand constant mechanical deformations, e.g., due to strains generated by cells that exert forces on their local environments as well as by exogenous forces that affect the entire biomaterial. The hybrid hydrogels are highly compatible with a number of different cell types, such as endothelial cells, neuronal cells, and macrophages, and allow for their cultivation for multiple days. Controlled degradation by proteases into nontoxic metabolites is crucial for in vivo applications, e.g., by providing a matrix that cells can actively remodel during culture or to regulate the release of cargo molecules in vivo. Together with the opportunity to conveniently introduce new functions by coassembly of modified depsi peptides, the material offers great potential as a regenerative scaffold for biomedicine.

Supporting Information

Supporting Information is available from the Wiley Online Library or from the author.

Acknowledgements

The authors are grateful to Jürgen Groll for the idea to apply peptide fibrils as gelators. The authors thank Raphaela L. Thierer, J. Luisa. J. L. L. Wiechmann, Markus Lamla, Andreas Riegger, and Nicole Kirsch-Pietz for experimental support and revising the manuscript. Andreas Hanewald and Kaloian Koynov helped with obtaining and discussing rheological data. The study was funded by the Baden-Württemberg Stiftung (BioMatS-15), by the Horizon 2020 project "AD GUT" (No. 686271), and by the Volkswagen foundation project 89943. C.V.S. gratefully acknowledges support through a Feodor Lynen Return Fellowship by the Humboldt Foundation. The work by B.K. was supported by the Deutsche Forschungsgemeinschaft through the CRC 1149 and grant KN543/6. Further, B.K. was supported by the Paul und Marlene Hepp-Stiftung and an Ulm University and German Army Hospital research initiative (U2.1d E/U2AD/ED002/EF550). The work by H.B. was supported by the CRC 1149 (project A04). The human umbilical vein endothelial cells used in this work were purchased from Lonza. All experiments were in accordance with institutional regulations by the local animal ethical committee (Regierungspräsidium Tübingen, Germany).

Conflict of Interest

The authors declare no conflict of interest.

Keywords

cell cultivation, depsi peptide, hydrogels, peptide nanofibers, thixotropy

Received: August 2, 2018
Revised: September 19, 2018
Published online: November 9, 2018

[1] a) C. Frantz, K. M. Stewart, V. M. Weaver, *J. Cell Sci.* **2010**, *123*, 4195; b) R. O. Hynes, *Science* **2009**, *326*, 1216.
[2] J. Thiele, Y. Ma, S. M. C. Bruekers, S. Ma, W. T. S. Huck, *Adv. Mater.* **2014**, *26*, 125.
[3] a) N. Annabi, A. Tamayol, J. A. Uquillas, M. Akbari, L. E. Bertassoni, C. Cha, G. Camci-Unal, M. R. Dokmeci, N. A. Peppas, A. Khademhosseini, *Adv. Mater.* **2014**, *26*, 85; b) E. Aurand, J. Wagner, C. Lanning, K. Bjugstad, *J. Funct. Biomater.* **2012**, *3*, 839.
[4] a) C. Li, A. Faulkner-Jones, R. Dun Alison, J. Jin, P. Chen, Y. Xing, Z. Yang, Z. Li, W. Shu, D. Liu, R. Duncan Rory, *Angew. Chem., Int. Ed.* **2015**, *54*, 3957; b) H. Onoe, T. Okitsu, A. Itou, M. Kato-Negishi, R. Gojo, D. Kiriya, K. Sato, S. Miura, S. Iwanaga, K. Kuribayashi-Shigetomi, Y. T. Matsunaga, Y. Shimoyama, S. Takeuchi, *Nat. Mater.* **2013**, *12*, 584.
[5] a) V. Slaughter Brandon, S. Khurshid Shahana, Z. Fisher Omar, A. Khademhosseini, A. Peppas Nicholas, *Adv. Mater.* **2009**, *21*, 3307; b) J. Boekhoven, S. I. Stupp, *Adv. Mater.* **2014**, *26*, 1642.

[6] a) J. B. Matson, S. I. Stupp, *Chem. Commun.* **2012**, *48*, 26; b) R. Ravichandran, M. Griffith, J. Phopase, *J. Mater. Chem. B* **2014**, *2*, 8466.

[7] a) M. Zhou, A. M. Smith, A. K. Das, N. W. Hodson, R. F. Collins, R. V. Ulijn, J. E. Gough, *Biomaterials* **2009**, *30*, 2523; b) T. Liebmann, S. Rydholm, V. Akpe, H. Brismar, *BMC Biotechnol.* **2007**, *7*, 88; c) Y. Yanlian, K. Ulung, W. Xiumei, A. Horii, H. Yokoi, Z. Shuguang, *Nano Today* **2009**, *4*, 193; d) J. D. Hartgerink, E. Beniash, S. I. Stupp, *Science* **2001**, *294*, 1684.

[8] a) S. S. Lee, T. Fyrner, F. Chen, Z. Álvarez, E. Sleep, D. S. Chun, J. A. Weiner, R. W. Cook, R. D. Freshman, M. S. Schallmo, K. M. Katchko, A. D. Schneider, J. T. Smith, C. Yun, G. Singh, S. Z. Hashmi, M. T. McClendon, Z. Yu, S. R. Stock, W. K. Hsu, E. L. Hsu, S. I. Stupp, *Nat. Nanotechnol.* **2017**, *12*, 821; b) T.-Y. Cheng, M.-H. Chen, W.-H. Chang, M.-Y. Huang, T.-W. Wang, *Biomaterials* **2013**, *34*, 2005; c) A. N. Edelbrock, Z. Àlvarez, D. Simkin, T. Fyrner, S. M. Chin, K. Sato, E. Kiskinis, S. I. Stupp, *Nano Lett.* **2018**, *18*, 6237.

[9] M. Zelzer, S. J. Todd, A. R. Hirst, T. O. McDonald, R. V. Ulijn, *Biomater. Sci.* **2013**, *1*, 11.

[10] a) M. Liu, X. Zeng, C. Ma, H. Yi, Z. Ali, X. Mou, S. Li, Y. Deng, N. He, *Bone Res.* **2017**, *5*, 17014; b) L. Taylor Danielle, M. in het Panhuis, *Adv. Mater.* **2016**, *28*, 9060.

[11] a) H. Tan, C. M. Ramirez, N. Miljkovic, H. Li, J. P. Rubin, K. G. Marra, *Biomaterials* **2009**, *30*, 6844; b) G. Liu, Q. Yuan, G. Hollett, W. Zhao, Y. Kang, J. Wu, *Polym. Chem.* **2018**, *9*, 3436; c) C. Cheng, X. Zhang, Y. Meng, Z. Zhang, J. Chen, Q. Zhang, *Soft Matter* **2017**, *13*, 3003.

[12] D. E. Clarke, E. T. Pashuck, S. Bertazzo, J. V. M. Weaver, M. M. Stevens, *J. Am. Chem. Soc.* **2017**, *139*, 7250.

[13] S. Mariusz, K. Yoshiaki, *Curr. Med. Chem.* **2007**, *14*, 2813.

[14] a) N. Amdursky, Y. Erez, D. Huppert, *Acc. Chem. Res.* **2012**, *45*, 1548; b) M. Biancalana, S. Koide, *Biochim. Biophys. Acta, Proteins Proteomics* **2010**, *1804*, 1405; c) S. G. Bolder, L. M. C. Sagis, P. Venema, E. van der Linden, *Langmuir* **2007**, *23*, 4144; d) S. Freire, M. H. de Araujo, W. Al-Soufi, M. Novo, *Dyes Pigm.* **2014**, *110*, 97.

[15] a) V. Cabiaux, R. Brasseur, R. Wattiez, P. Falmagne, J. M. Ruysschaert, E. Goormaghtigh, *J. Biol. Chem.* **1989**, *264*, 4928; b) E. Goormaghtigh, V. Cabiaux, J.-M. Ruysschaert, *Eur. J. Biochem.* **1990**, *193*, 409; c) D. M. Byler, H. Susi, *Biopolymers* **1986**, *25*, 469.

[16] K. Eisele, R. A. Gropeanu, C. M. Zehendner, A. Rouhanipour, A. Ramanathan, G. Mihov, K. Koynov, C. R. W. Kuhlmann, S. G. Vasudevan, H. J. Luhmann, T. Weil, *Biomaterials* **2010**, *31*, 8789.

[17] a) J. Gačanin, A. Kovtun, S. Fischer, V. Schwager, J. Quambusch, L. Kuan Seah, W. Liu, F. Boldt, C. Li, Z. Yang, D. Liu, Y. Wu, T. Weil, H. Barth, A. Ignatius, *Adv. Healthcare Mater.* **2017**, *6*, 1700392; b) Y. Wu, C. Li, F. Boldt, Y. Wang, S. L. Kuan, T. T. Tran, V. Mikhalevich, C. Förtsch, H. Barth, Z. Yang, D. Liu, T. Weil, *Chem. Commun.* **2014**, *50*, 14620.

[18] a) A. J. Engler, S. Sen, H. L. Sweeney, D. E. Discher, *Cell* **2006**, *126*, 677; b) R. Uibo, I. Laidmäe, E. S. Sawyer, L. A. Flanagan, P. C. Georges, J. P. Winer, P. A. Janmey, *Biochim. Biophys. Acta, Mol. Cell Res.* **2009**, *1793*, 924.

[19] T. G. Mezger, *The Rheology Handbook*, Vincentz Network GmbH & Co KG, Hanover, Germany **2006**.

[20] a) K.-I. Sano, R. Kawamura, T. Tominaga, N. Oda, K. Ijiro, Y. Osada, *Biomacromolecules* **2011**, *12*, 4173; b) Z. Wei, J. H. Yang, Z. Q. Liu, F. Xu, J. X. Zhou, M. Zrínyi, Y. Osada, Y. M. Chen, *Adv. Funct. Mater.* **2015**, *25*, 1352; c) Z. Wei, J. H. Yang, J. Zhou, F. Xu, M. Zrínyi, P. H. Dussault, Y. Osada, Y. M. Chen, *Chem. Soc. Rev.* **2014**, *43*, 8114.

[21] a) L. Aulisa, H. Dong, J. D. Hartgerink, *Biomacromolecules* **2009**, *10*, 2694; b) M. K. Włodarczyk-Biegun, K. Farbod, M. W. T. Werten, C. J. Slingerland, F. A. de Wolf, J. J. J. P. van den Beucken, S. C. G. Leeuwenburgh, M. A. Cohen Stuart, M. Kamperman, *PLoS One* **2016**, *11*, e0155625; c) S. Mukherjee, M. R. Hill, B. S. Sumerlin, *Soft Matter* **2015**, *11*, 6152.

[22] V. Breedveld, A. P. Nowak, J. Sato, T. J. Deming, D. J. Pine, *Macromolecules* **2004**, *37*, 3943.

[23] a) M. C. Bastings Maartje, S. Koudstaal, E. Kieltyka Roxanne, Y. Nakano, A. C. H. Pape, A. M. Feyen Dries, J. van Slochteren Frebus, A. Doevendans Pieter, P. G. Sluijter Joost, E. W. Meijer, A. J. Chamuleau Steven, Y. W. Dankers Patricia, *Adv. Healthcare Mater.* **2014**, *3*, 70; b) T. Nonoyama, H. Ogasawara, M. Tanaka, M. Higuchi, T. Kinoshita, *Soft Matter* **2012**, *8*, 11531; c) X. Zhang, X. Chu, L. Wang, H. Wang, G. Liang, J. Zhang, J. Long, Z. Yang, *Angew. Chem., Int. Ed.* **2012**, *51*, 4388.

[24] J. Nanda, A. Biswas, A. Banerjee, *Soft Matter* **2013**, *9*, 4198.

[25] a) S. M. Bleay, C. B. Loader, V. J. Hawyes, L. Humberstone, P. T. Curtis, *Composites, Part A* **2001**, *32*, 1767; b) D. Coillot, F. O. Méar, R. Podor, L. Montagne, *Adv. Funct. Mater.* **2010**, *20*, 4371; c) K. Haraguchi, K. Uyama, H. Tanimoto, *Macromol. Rapid Commun.* **2011**, *32*, 1253; d) J. Liu, G. Song, C. He, H. Wang, *Macromol. Rapid Commun.* **2013**, *34*, 1002; e) S. R. White, N. R. Sottos, P. H. Geubelle, J. S. Moore, M. R. Kessler, S. R. Sriram, E. N. Brown, S. Viswanathan, *Nature* **2001**, *409*, 794.

[26] E. Sleep, B. D. Cosgrove, M. T. McClendon, A. T. Preslar, C. H. Chen, M. H. Sangji, C. M. R. Pérez, R. D. Haynes, T. J. Meade, H. M. Blau, S. I. Stupp, *Proc. Natl. Acad. Sci.* **2017**, *114*, E7919.